The Pharma Innovation Journal 2016; 5(5): 01-08

www.ThePharmaJournal.com

The Pharma Innovation

ISSN: 2277- 7695
TPI 2016; 5(5): 01-08

ICV Factor: 6.79
www.thepharmajournal.com
Received: 10-02-2016
Accepted: 13-03-2016

Dr D N Tibarewala
Professor, School of Biosciences and Engineering, Jadavpur University, Kolkata, India

Dr Partha Majumder
Biomedical Scientist & Systems Biologist, Former Principal Scientist (Helixinfosystems, Chennai), Former Head of The Department of Applied Biotechnology & Bioinformatics, Sikkim Manipal University, CC: 1637, Kolkata, India.

Dr Anjana Mazumdar
Professor, Department of Oral Pathology, Dr. R. Ahmed Govt. Dental College, Kolkata, India

Dr Sukumar Roy
Professor & Head, Department of Biomedical Engineering, Netaji Subhas Engineering College, Garia, Kolkata, India

Dr Veera Talukdar
Assistant Professor, MK College of science and commerce, Mumbai

Corresponding Author
Dr Partha Majumder
Biomedical Scientist & Systems Biologist, Former Principal Scientist (Helixinfosystems, Chennai), Former Head of The Department of Applied Biotechnology & Bioinformatics, Sikkim Manipal University, CC: 1637, Kolkata, India

Egfr Augments Aerobic Glycolysis In Multi-Negetive Breast Cancer Cells to Promote Tumorigenesis and Immune Escape

Dr D N Tibarewala, Dr Partha Majumder, Dr Anjana Mazumdar, Dr Sukumar Roy, Dr Veera Talukdar

Abstract
Cellular metabolism and bioenergetics are regulated by cancer genes and are intimately linked to the growth and survival of cancer cells. Metabolism generates oxygen radicals, which contribute to oncogenic mutations. Activated oncogenes and loss of tumor suppressors in turn alter metabolism and induce aerobic glycolysis. Aerobic glycolysis or the Warburg effect links the high rate of glucose fermentation to cancer. Together with glutamine, glucose via glycolysis provides the carbon skeletons, NADPH, and ATP to build new cancer cells, which persist in hypoxia that in turn rewires metabolic pathways for cell growth and survival. Excessive caloric intake is associated with an increased risk for cancers, while caloric restriction is protective, perhaps through clearance of mitochondria or mitophagy, thereby reducing oxidative stress. Hence, the links between metabolism and cancer are multifaceted, spanning from the low incidence of cancer in large mammals with low specific metabolic rates to altered cancer cell metabolism resulting from mutated enzymes or cancer genes.

Keywords: caloric restriction, cancer, glycolysis, metabolism, oncogenes, tumor suppressors

Introduction
Accelerated glycolysis is a common feature of rapidly proliferating cancer cells. Unlike normal differentiated cells, most cancer cells produce large amounts of lactate regardless of oxygen levels. This metabolic property is often referred to as "aerobic glycolysis" [1, 2], a well-known metabolic reprogramming of cancer cells to sustain cell proliferation and a hallmark of cancer [3]. In cancer cells, oncogenic receptor tyrosine kinase (RTK) signaling participates in metabolic reprogramming and stimulates the accumulation of cellular metabolites, which are then used as building blocks for cell growth [4]. Thus, understanding the cross-regulation between RTK signaling and metabolites and/or metabolic enzymes of glycolysis may shed light on new regulation of cancer cell metabolism.
Hexokinase (HK) and pyruvate kinase (PK) are two key enzymes regulating two irreversible steps in glycolysis. HK isozymes 1–4 catalyze the phosphorylation of glucose, which is the first of the two irreversible steps in glycolysis. Although HK2 is associated with cancer promotion and has been proposed as a potential therapeutic target, the detailed molecular mechanisms are not fully understood [5, 6]. PK catalyzes the dephosphorylation of phosphoenolpyruvate to pyruvate, which is the last irreversible step of glycolysis, and the expression of PK is frequently altered during tumorigenesis [7]. The M1 isoform of PK (PKM1) is expressed in most adult tissues, whereas M2 (PKM2) is exclusively expressed during embryonic development [8, 9]. Notably, most tumor cells reexpress PKM2, suggesting that the switch from PKM1 to PKM2 leads to aerobic glycolysis, which provides a selective growth advantage *in vivo* [7] cancer cells have the ability to disengage immune response by inactivating cytotoxic T-cell function via secretion of cytokine or immune checkpoint proteins. Interestingly, metabolic regulation has been reported to play an important role in T-cell differentiation and functions. For instance, Myc and HIF1α, which are well-known regulators of metabolism, stimulate T-cell receptor activation. Moreover, several glycolytic and TCA cycle metabolites, for example, glucose, acetyl-CoA, and lactate, also regulate T-cell proliferation and functions. Nonetheless, the link connecting oncogenic signaling, metabolism, and immune escape in cancer cells has not been well established.
The EGFR is one of the major regulators of cell proliferation, cell survival, and metabolism. In triple-negative breast cancer (TNBC) patients, EGFR overexpression is frequently observed

and associated with poor clinical outcome. TNBC, which accounts for approximately 15% to 20% of breast cancers in the United States, lacks the expression of estrogen receptor (ER) and progesterone receptor (PR) as well as amplification of HER2/neu and is associated with poorer outcome compared with other breast cancer subtypes Unlike ER-positive, PR-positive, or HER2-overexpressing tumors, the lack of well-defined molecular targets and the heterogeneity of the disease pose a challenge in TNBC treatment Clinical outcomes for anti-EGFR targeted therapy in breast cancer have been disappointing compared with those in lung, colon, and head and neck cancers suggesting that cancer-specific mechanisms or biologic functions of EGFR have yet to be discovered in TNBC.

EGF is known to accelerate glucose consumption and lactate production in cancer cells, including breast cancer In addition, EGF-stimulated nuclear translocation of PKM2 promotes tumorigenesis and cell proliferation of glioma cells Although it has been known for two decades that EGF stimulation leads to a high rate of glycolysis in cells, how this is directly linked to EGFR is not clear yet. Here, we report an EGF/EGFR/fructose-1, 6-bisphosphate (F1,6BP) signaling axis in TNBC cells that increases lactate production, which promotes immune evasion. Our findings provide a rationale for combining EGFR tyrosine kinase inhibitor, gefitinib, with glycolysis inhibitor, 2-deoxy-d-glucose (2-DG), as a potential therapeutic strategy for TNBC.

Materials and Methods

Cell culture and treatment

Breast cancer cell lines MDA-MB-468, BT549, HS578T, BT20, MDA-MB-231, MDA-MB-436, HBL100, AU565, SKBR3, MCF7, T47D, ZR75-1, and human embryonic kidney cell line HEK 293T cells were obtained from ATCC. Cell lines were validated by short tandem repeat DNA fingerprinting using the AmpFlSTR Identifiler PCR Amplification Kit (Applied Biosystems catalog no. 4322288; Life Technologies) according to the manufacturer's instructions. Cells were grown in DMEM supplemented with 10% FBS. EGF (Sigma-Aldrich) was prepared according to the manufacturers' instructions. Cells were treated with 25 ng/mL EGF. Gefitinib (5 μmol/L) was used to inhibit EGFR kinase activity.

Western blot analysis, immunocytochemistry, immunoprecipitation, and IHC staining

Western blot analysis, immunoprecipitation, and immunocytochemistry were performed as described previously. Antibody information is described in the Supplementary Table S3. Image acquisition and quantitation of band intensity were performed using Odyssey infrared imaging system (LI-COR Biosciences). IHC staining was performed as previously described. To validate the specificity of phospho-Y148-PKM2 antibody in IHC, we performed peptide competition assay by staining human breast tumor sample with phospho-Y148-PKM2 antibody blocked with mock or phospho-Y148-PKM2-peptide or nonphospho-Y148-PKM2-peptide. Duolink II fluorescence assay was performed as described by the manufacturer (Olink Bioscience). *In vitro* kinase assays were performed as described in Supplementary Information.

Generation of stable cells using lentiviral infection

Human PKM2 ORF clone was obtained from the shRNA/ORF Core Facility (MD Anderson Cancer Center, Houston, TX) and cloned into pCDH lentiviral expression vector to establish Flag-PKM2 expression cell lines. The lentiviral-based shRNA (pGIPZ plasmids) used to knockdown expression of PKM2 was purchased from the shRNA/ORF Core Facility (MD Anderson Cancer Center, Houston, TX). pGIPZ-shPKM2/Flag-PKM2 dual-expression construct to knock down endogenous PKM2 and to reconstitute Flag-PKM2 (by creating a silent mutant that is resistant to shPKM2) was performed as described in Supplementary Information.

Orthotopic xenograft breast cancer model and treatment

All animal procedures were conducted under the guidelines approved by the Institutional Animal Care and Use Committee at MD Anderson Cancer Center. Female Nu/Nu nude and BALB/c mice were used as hosts for tumor xenografts and 4T1 syngeneic model, respectively. Briefly, orthotopic breast cancer mouse model was established as previously described For MDA-MB-468 $PKM2^{WT}$ and $PKM2^{Y148F}$ cells, 1×10^6 cells in 50 μL medium mixed with 50 μL Matrigel (BD Biosciences) were injected into the left and right mammary fat pad, respectively. For 4T1 syngeneic model, $PKM2^{WT}$- and $PKM2^{Y148F}$-expressing mouse 4T1-luc cells (5×10^4 cells in 50 μL medium mixed with 50 μL Matrigel) were injected to the mammary fat pad. Tumor was measured weekly with a caliper, and tumor volume was calculated by the formula: $\pi/6 \times \text{length} \times \text{width}^2$. For drug treatment, mice were treated with daily oral doses 500 mg/kg 2-DG and 10 mg/kg gefitinib for 2 weeks (5 days/week). Tumor infiltration lymphocyte profiles in excised tumors were analyzed as described in Supplementary Information.

T cell–mediated tumor cell killing assay

T cell–mediated tumor cell killing assay was performed according to the manufacturer's protocol (Essen Bioscience). To analyze the killing of tumor cells by T-cell inactivation, nuclear-restricted red fluorescent protein (RFP)-expressing tumor cells were cocultured with activated primary human T cells (Stemcell Technologies) in the presence of caspase 3/7 substrate (Essen Bioscience). T cells were activated by incubation with anti-CD3 antibody (100 ng/mL) and IL2 (10 ng/mL). After 96 hours, RFP and green fluorescent (NucView 488 Caspase 3/7 substrate) signals were measured. Green fluorescent cells were counted as dead cells. Coculture of Jurkat T cells and tumor cells was performed as described previously. Secreted IL2 level in medium was measured according to the manufacturer's protocol (Human IL2 ELISA Kits, Thermo Fisher Scientific).

qRT-PCR assays

qRT-PCR assays were performed to measure the expression of mRNA and mature miRNAs as previously described. To measure the expression of mRNA or miRNAs, cDNA was synthesized from 1 μg purified total RNA by SuperScript III cDNA synthesis system using random hexamers (Invitrogen) according to the manufacturer's instructions. For detection of mature miRNAs, TaqMan MicroRNA Assay kits for hsa-miR-143, hsa-miR-125a, and hsa-miR-125b (Applied Biosystems) were used following the manufacturer's protocol. All data analysis was performed using the comparative C_t method. Results were normalized to the internal control β-actin mRNA or U6 snRNA.

ECAR/OCR, lactate, pyruvate kinase activity, and glucose uptake measurement

Extracellular acidification rate (ECAR) and oxygen consumption rate (OCR) were measured using extracellular flux analyzer (XF96) analyzer (Seahorse Bioscience) as described by the manufacturer. More details can be found in Supplementary Information. Lactate production (Lactate Assay Kit) and pyruvate kinase activity (Pyruvate Activity Assay Kit) were measured as described by the manufacturer (BioVision). To measure glucose uptake, cells were incubated with a fluorescent D-glucose derivative, 2-[*N*-(7-nitrobenz-2-oxa-1,3-diazol-4-yl)amino]-2-deoxy-d-glucose (2-NBDG; Invitrogen) for 10 minutes after EGF and/or gefitinib treatment. The fluorescence intensity of 2-NBDG was measured using a microplate reader Synergy H4 (BioTeK) and normalized to that of 2-NBDG by total protein amount.

Mass spectrometry

Mass spectrometric analysis for protein identification was performed as previously described. To identify PKM2 phosphorylation sites, we purified FLAG-PKM2 with M2 resin (Sigma) that coexpressed with EGFR in 293T cells and analyzed the results by SDS–PAGE and Western blot analysis. The protein band corresponding to PKM2 was excised and subjected to in-gel digestion with trypsin. Samples were analyzed by nanoelectrospray mass spectrometry, using an Ultimate capillary LC system (LC Packings) coupled to a QSTARXL quadrupole time-of-flight mass spectrometer (Applied Biosystems/MDS Sciex).

LC/MS-MS metabolomic analysis

LC/MS-MS metabolomic analysis was performed from dried samples reconstituted in 100 µL 5 mmol/L ammonium acetate in 95% water/5% acetonitrile + 0.5% acetic acid prior to LC/MS analysis. More details can be found in Supplementary Information.

Statistical analysis

Data in bar graphs represent mean fold change relative to untreated or control groups with SD of three independent experiments. Statistical analyses were performed using SPSS (Ver. 20, SPSS Inc.). The correlation between protein expression and TNBC subset was analyzed using Spearman correlation and Mann–Whitney test. Student *t* test was performed for experimental data. A P value < 0.05 was considered statistically significant. Asterisk indicates statistically significant by Student *t* test. All error bars are expressed as ±SD of three independent experiments.

Results

EGF signaling stimulates glycolysis in TNBC cells

To test whether EGF affects glycolysis or mitochondrial respiration through EGFR, we measured the metabolic profile of an EGFR-overexpressing breast cancer cell line MDA-MB-468. Under EGF stimulation, these cells showed higher glycolytic activities, as indicated by the increased ECAR, which was attenuated by cotreatment with EGFR-tyrosine kinase inhibitor (TKI) gefitinib (Fig. 1A). In contrast, EGF had no effect on glycolysis in low EGFR-expressing MCF7 breast cancer cells (Fig. 1B). We also measured the OCR and lactate production in MDA-MB-468 and MCF7 cells. We did not observe any differences in OCR (Fig. 1C and D); however, lactate production (Fig. 1E and F) and glucose uptake (Supplementary Fig. S1A) increased only in MDA-MB-468 cells, and the addition of gefitinib eliminated the differences. Both The Cancer Genome Atlas (TCGA) database (patient samples; Fig. 1G and Supplementary Fig. S1B) and Western blot (cell lines; Supplementary Fig. S1C) analyses indicated higher EGFR expression in TNBC than in non-TNBC, and therefore we further analyzed the changes in glycolysis in TNBC and non-TNBC cell lines under EGF stimulation. Similar to the results observed in MDA-MB-468 and MCF7 cells, five TNBC and one non-TNBC cell line expressing EGFR also had increased glycolysis and lactate production but not OCR under EGF treatment (Supplementary Fig. S1D). To measure the relative contribution of glycolysis and mitochondrial respiration in energy production, we compared the OCR to ECAR ratio in nine breast cancer cell lines and found that TNBC cell lines exhibited more glycolytic phenotype compared with non-TNBC cell lines (Fig. 1H), indicating that EGF signaling enhances glycolysis but not oxidative phosphorylation in TNBC cells. In addition, other EGFR-expressing cancer cells, such as A431 and SW48, also showed enhanced aerobic glycolysis by EGF treatment (Supplementary Fig. S1E). Together, these results implied that EGF signaling specifically stimulates aerobic glycolysis in EGFR-expressing cancer cells. EGFR is highly expressed in TNBC, for which no effective clinical treatment is currently available. Therefore, all subsequent investigations focused on EGFR-expressing TNBC cells although the outcome may apply to other EGFR-expressing cancer cells.

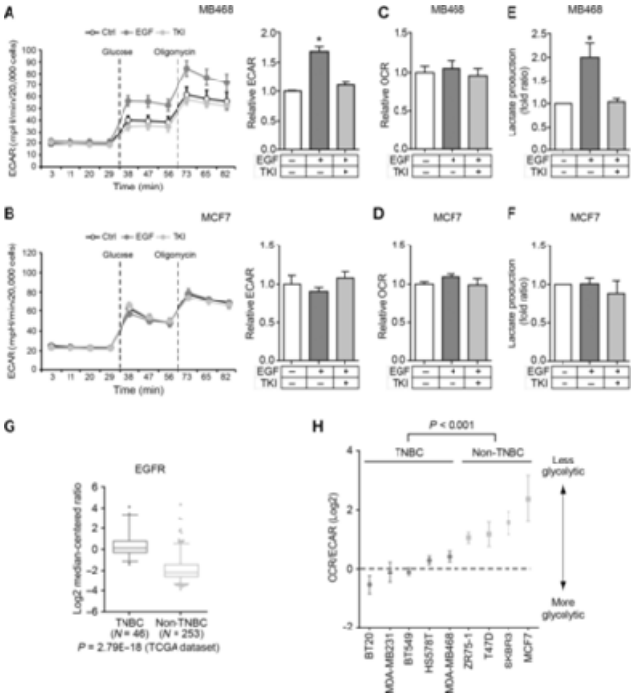

Fig 1: *EGF signaling stimulates glycolysis in TNBC cells. A and B, ECAR, an indicator of glycolysis, was measured in MDA-MB-468 (A) or MCF7 (B) cells following the addition of glucose (10 mmol/L) or oligomycin (1 µmol/L) in the presence of EGF and/or TKI. Right, relative ECAR of EGFR before and after glucose injection. Ctrl, nontreated control cells; EGF, EGF-treated cells; TKI, EGF and TKI cotreated cells. C and D, OCR was measured in MDA-MB-468 (C) or MCF7 (D) following the addition of oligomycin (1 µmol/L) or FCCP (0.5 µmol/L) in the presence of EGF and/or TKI. E and F, lactate production was measured in the medium of MDA-MB-468 (E) or MCF7 (F) cells treated with EGF and/or TKI. G, a box-and-whisker plot of EGFR mRNA expression in TNBC and non-TNBC tumors from*

the TCGA dataset using Oncomine. H, OCR/ECAR values in breast cancer cell lines following the addition of oligomycin (1 µmol/L).

EGFR binds to and phosphorylates PKM2 to inhibit its activity

To understand how EGFR regulates glycolysis, we analyzed the EGFR-binding proteins that we previously reported using Ingenuity Pathway Analysis and identified four glycolytic proteins: HK1, phosphofructokinase, GAPDH, and PKM2. We then validated their interaction with EGFR by endogenous coimmunoprecipitation followed by Western blot analysis and demonstrated that HK1 and PKM2 interacted specifically with EGFR (Supplementary Fig. S2A). However, only the interaction between PKM2 and EGFR was increased by EGF and inhibited by gefitinib as shown by coimmunoprecipitation (Fig. 2A and C) and Duolink assay (Fig. 2B and D and Supplementary Fig. S2B). These results indicate that PKM2 is a novel binding partner of EGFR.

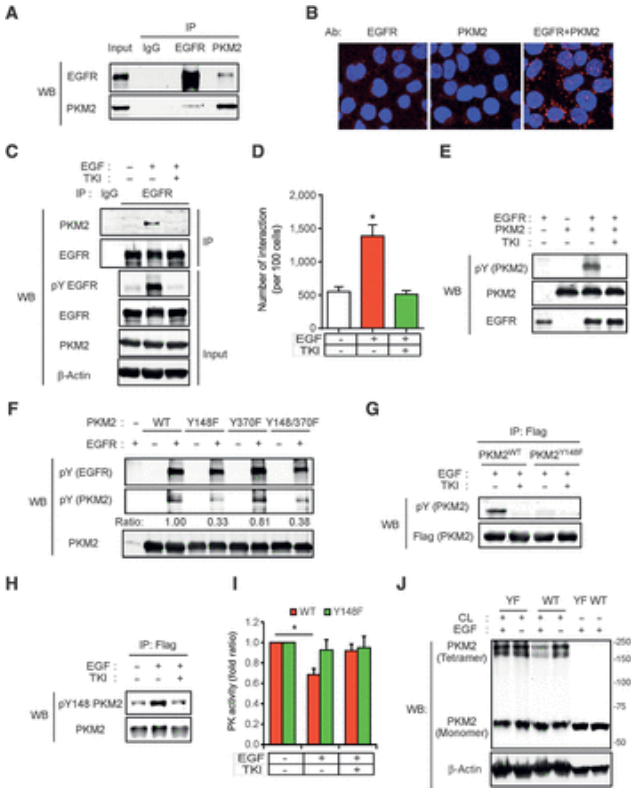

Fig 2: *EGFR binds to and phosphorylates PKM2 to inhibit its activity. A, lysates from EGF-treated MDA-MB-468 cells were subjected to coimmunoprecipitation using EGFR and PKM2 antibodies followed by Western blotting. IgG, negative control. B, EGF-treated MDA-MB-468 cells were immunostained with EGFR and/or PKM2 antibodies and assessed using Duolink II assay as indicated. Red foci indicate interactions between endogenous EGFR and PKM2 proteins. EGFR or PKM2 antibody staining alone served as negative control. C, lysates from EGF- and/or TKI-treated MDA-MB-468 cells were subjected to immunoprecipitation using EGFR antibody followed by Western blotting. IgG, negative control. D, EGF- and/or TKI-treated MDA-MB-468 cells were immunostained with EGFR and PKM2 antibodies and then subjected to Duolink II assay. The number of red foci as described in B was calculated on the basis of three randomly selected fields and normalized by nuclear number (per 100 cells). E, in vitro kinase assay was performed using purified full-length recombinant His-PKM2 and commercially available purified EGFR. PKM2 phosphorylation was detected by phospho-Tyr antibody. F, in vitro kinase reaction products of mutant PKM2 Y148F and/or Y370F detected by phospho-Tyr antibody. G, EGF- and/or TKI-treated Flag-PKM2^{WT}- or PKM2^{Y148F}-expressing MDA-MB-468 cells were immunoprecipitated with Flag M2 affinity resin. Flag-PKM2 proteins were eluted by Flag peptide followed by Western blotting. H, Flag-PKM2^{WT}-expressing MDA-MB-468 cells were treated with EGF and/or TKI and were immunoprecipitated with Flag M2 affinity resin. Flag-PKM2 proteins were eluted by Flag peptide followed by Western blotting using phospho-Y148 PKM2 antibody. I, PK activities of Flag-PKM2^{WT}- or PKM2^{Y148F}-expressing MDA-MB-468 cells treated with EGF and/or TKI. J, EGF-treated Flag-PKM2^{WT}- or PKM2^{Y148F}-expressing MDA-MB-468 cells were cross-linked by glutaraldehyde followed by Western blotting. CL, cross-linker glutaraldehyde.*

The interaction between EGFR and PKM2 prompted us to ask whether PKM2 is a phosphorylation substrate of EGFR. As shown in Fig. 2E, PKM2 can be phosphorylated by commercially available purified EGFR protein, and this phosphorylation was abolished by gefitinib treatment. To determine the phosphorylation site(s), a MS/MS analysis was performed, which identified two PKM2 Tyr phosphorylation sites (Y148 and Y370) in EGF-treated cells (Supplementary Fig. S2C). To further characterize these two sites, we generated three PKM2 mutants, PKM2 Y148F, PKM2 Y370F, and PKM2 Y148F/Y370F. Interestingly, phosphorylation of PKM2 Y148F but not Y370F mutant was significantly decreased compared with PKM2 wild type (WT) by an *in vitro* EGFR kinase assay (Fig. 2F). To measure PKM2 Y148 phosphorylation *in vivo*, we first established PKM2 WT (PKM2^{WT}) or Y148F mutant (PKM2^{Y148F}) in PKM2-knockdown MDA-MB-468 cells by using a dual-expression construct to knockdown endogenous PKM2 by shRNA and then reexpress exogenous Flag-PKM2 (Supplementary Fig. S2D). As expected, phosphorylation of PKM2 was readily detectable in PKM2^{WT}-expressing cells and blocked by gefitinib, but not in PKM2^{Y148F}-expressing cells (Fig. 2G). A phospho-Y148 PKM2 antibody that we generated preferentially recognized phospho-PKM2^{WT} but not PKM2^{Y148F} (Fig. 2H and Supplementary Fig. S2E–S2G), indicating that Y148 is a major EGFR phosphorylation site. Interestingly, EGF treatment decreased the PK activity of PKM2 and of its tetramer, an active form of PKM2 in PKM2^{WT}-expressing but not in PKM2^{Y148F}-expressing PKM2-knockdown MDA-MB-468 cells (Fig. 2I and J and Supplementary S2H). Together these data suggest that EGFR phosphorylation of PKM2 at Y148 reduces active PKM2 tetramer and inhibits its PK activity.

EGF signaling reprograms cancer cell metabolism by PKM2 phosphorylation

Next, we investigated whether EGFR-mediated phospho-Y148 PKM2 affects biologic activities, such as cell proliferation, *in vitro* and *in vivo*. Cell proliferation, glycolysis, and lactate production were higher in PKM2^{WT} than in PKM2^{Y148F} cells (Fig. 3A). Furthermore, tumor volumes derived from PKM2^{WT}-expressing BT549 or MDA-MB-468 cells were significantly larger compared with those expressing PKM2^{Y148F} (Fig. 3B and Supplementary Fig. S3A). As PKM2 regulates the last step of glycolysis, and decreased PKM2 activity leads to an accumulation of glycolytic intermediates and promotes tumor growth, we also profiled the intracellular glycolysis-related metabolites in EGF-treated PKM2^{WT} and PKM2^{Y148F} cells. Indeed, the levels of most glycolytic intermediates were higher in PKM2^{WT}-expressing MDA-MB-468 cells compared with those expressing PKM2^{Y148F} (Fig. 3C). To further determine the clinical relevance, we analyzed

the relationship between phosho-Y148 PKM2, EGFR, and proliferation marker Ki-67 in human breast cancer tissues by IHC staining. A positive correlation was identified between PKM2 Y148 phosphorylation, EGFR expression, and Ki67 in human TNBC but not in non-TNBC tissues (Fig. 3D and Supplementary Tables S1 and S2). High levels of phospho-PKM2 and EGFR also correlated with poorer survival in TNBC but not in non-TNBC patients (Fig. 3E and Supplementary Fig. S3B). Together, these results support that EGFR-induced phosphorylation at PKM2 Y148 confers a proliferation advantage in TNBC cells.

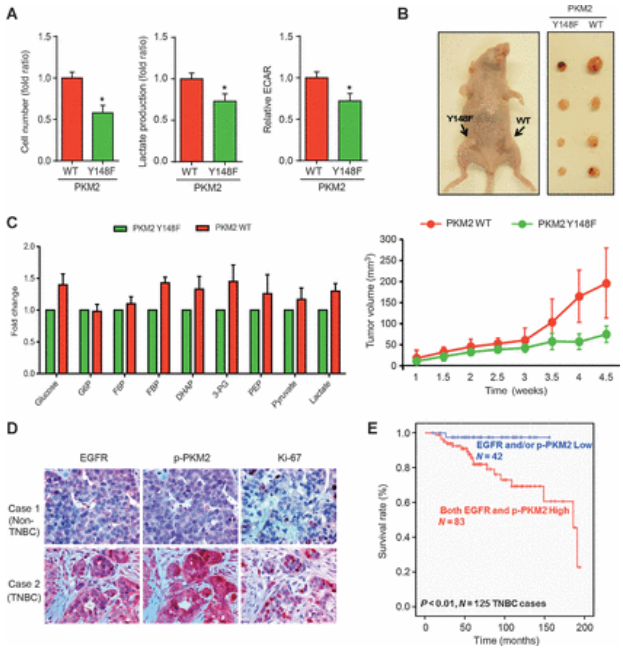

Fig 3: *EGFR reprograms cancer cell metabolism by PKM2 phosphorylation in TNBC cells. A, cell proliferation, glycolysis (ECAR), and lactate production were measured in EGF-treated PKM2^{WT}- or PKM2^{Y148F}-expressing MDA-MB-468 cells. B, nude mice were injected with PKM2^{WT}- and PKM2^{Y148F}-expressing BT549 cells in mammary glands as shown (top). Tumors were measured and dissected at the endpoint. Tumors were measured at the indicated time points. N = 8 per group (bottom). C, fold changes of glycolytic intermediates in EGF-treated MDA-MB-468 cells expressing PKM2^{WT} or PKM2^{Y148F}. 3-PG, 3-phosphoglyceric acid; DHAP, dihydroxyacetone phosphate; F6P, fructose 6-phosphate; G6P, glucose 6-phosphate; PEP, phosphoenolpyruvate. D, representative images of IHC staining of EGFR, phospho-Y148 PKM2, and Ki-67 in non-TNBC (case 1) and TNBC (case 2) tumor tissues. E, Kaplan–Meier survival curve of EGFR and phospho-PKM2 in TNBC tissues (N = 125, P < 0.01).*

Upregulation of HK2 expression by EGF signaling also enhances aerobic glycolysis

Knockdown of PKM2 abolished EGF-enhanced lactate production under short (2 hours) EGF treatment (Supplementary Fig. S4A). Unexpectedly, however, knocking down PKM2 did not abolish EGF-enhanced lactate production under longer (24 hours) EGF treatment (Supplementary Fig. S4A). Furthermore, the metabolic intermediates, such as amino acids and nucleotide precursors, were significantly increased in cells exposed to longer EGF treatment (Supplementary Fig. S4B and S4C). These results imply that other mechanisms at a later stage may also be involved in EGF signaling–induced aerobic glycolysis in addition to the early stage PKM2 phosphorylation. To identify these later-stage mechanisms, we asked whether the expression pattern of glycolytic enzymes correlated with EGFR expression in human breast cancer specimens. Analysis of TCGA database using Oncomine revealed that several glycolytic enzymes were significantly increased in TNBC tissues and positively correlated with EGFR expression (Supplementary Fig. S4D). To further validate these results, we analyzed mRNA expression of a number of glycolytic enzymes in EGF-treated TNBC and non-TNBC cells. Interestingly, the levels of mRNA and protein expression of HK2, but not HK1, were significantly increased by EGF treatment (24 hours) in both MDA-MB-468 and BT549 TNBC cells (Fig. 4A and B and Supplementary Fig. S4E and S4F). In addition, EGF stimulation also enhanced HK activity (Fig. 4C). From the TCGA dataset, HK2 expression, but not HK1, correlated with TNBC or EGFR expression (Fig. 4D and Supplementary Fig. S4G and S4H). Knocking down both PKM2 and HK2 had more reduction in EGF-induced lactate production than knocking down PKM2 or HK2 alone (Fig. 4E). These data suggested that both EGF-induced upregulation of HK2 and inhibition of PKM2 activity by phosphorylation enhance aerobic glycolysis.

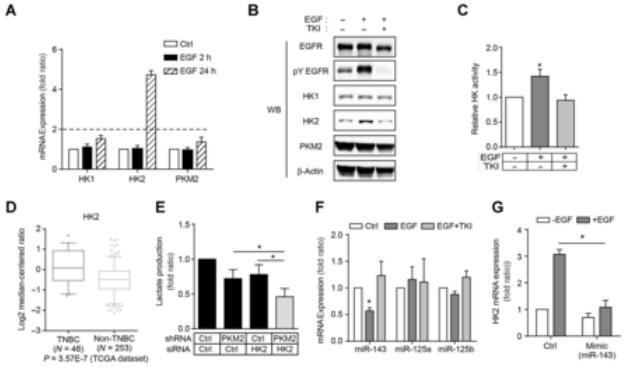

Fig 4: *Upregulation of HK2 expression by EGF signaling contributes to aerobic glycolysis in TNBC cells. A, the mRNA expression of HK1, HK2, and PKM2 in EGF-treated MDA-MB-468 cells. Ctrl, without EGF treatment. B, protein expression of HK1, HK2, and PKM2 in EGF-treated MDA-MB-468 cells. C, hexokinase activity was measured in MDA-MB-468 cells after 24-hour EGF treatment. D, a box-and-whisker plot of HK2 gene expression in TNBC and non-TNBC tumor tissues. E, lactate production of PKM2 and/or HK2 knockdown MDA-MB-468 cells after 24-hour EGF treatment. F, RT-qPCR analysis of miR-143, miR-125a, and miR-125b expression in EGF- and/or TKI-treated MDA-MB-468 cells. Ctrl, without EGF and/or TKI treatment. G, RT-qPCR analysis of HK2 mRNA expression in MDA-MB-468 cells transfected with miR-143 mimic or miRNA mimic negative control (ctrl) and treated with or without EGF for 24 hours.*

EGFR has recently been shown to regulate miRNA expression via Ago2 protein Therefore, we asked whether EGF-induced increased in HK2 might be regulated by miRNA. We analyzed the 3′-UTR of HK2 mRNA using TargetScan and identified three miRNAs, miR-143, miR-125a, and miR-125b, predicted to regulate HK2 mRNA. Among these, only expression of miR-143 was significantly decreased in EGF-treated MDA-MB-468 cells, which was restored by gefitinib treatment (Fig. 4F). Furthermore, addition of miR-143 mimic attenuated EGF-induced HK2 mRNA expression (Fig. 4G) but did not affect the level of pY EGFR expression (Supplementary Fig. S4I). Thus, EGF may upregulate HK2 expression by downregulating miR-143.

Glycolytic metabolite F1, 6BP binds directly to and enhances the activity of EGFR

The level of EGFR tyrosine phosphorylation was substantially reduced in PKM2^{Y148F}-expressing and PKM2-knockdown (shPKM2) MDA-MB-468 cells compared with those expressing PKM2^{WT} (Fig. 5A). However, there was no difference in EGFR phosphorylation when EGFR was incubated with PKM2 WT or PKM2 Y148F, suggesting that PKM2 did not directly phosphorylate EGFR (Supplementary Fig. S5A). We also noticed that the levels of several glycolysis metabolites were increased by EGF treatment in PKM2^{WT} but not PKM2^{Y148F} cells (Fig. 3C). Therefore, we asked whether enhanced EGFR phosphorylation was a result of the increase in the levels of these metabolites. Among them, only the addition of F1, 6BP to the culture medium increased EGFR tyrosine phosphorylation by more than 3-fold (Fig. 5B). Consistently, *in vitro* EGFR kinase assay and RTK array analysis also demonstrated enhanced EGFR tyrosine phosphorylation in the presence of F1,6BP (Fig. 5C and D and Supplementary Fig. S5B and S5C). Unlike F1,6BP, fructose-6-phosphate (F6P), which is structurally similar to F1,6BP, did not affect EGFR tyrosine phosphorylation (Fig. 5B and D). In addition, ^{14}C-labeled F1,6BP bound to the intracellular domain (ICD) of EGFR protein, which was blocked by nonlabeled F1,6BP (Fig. 5E and Supplementary Fig. S5D). These results suggested that F1,6BP binds directly to EGFR to enhance its phosphorylation.

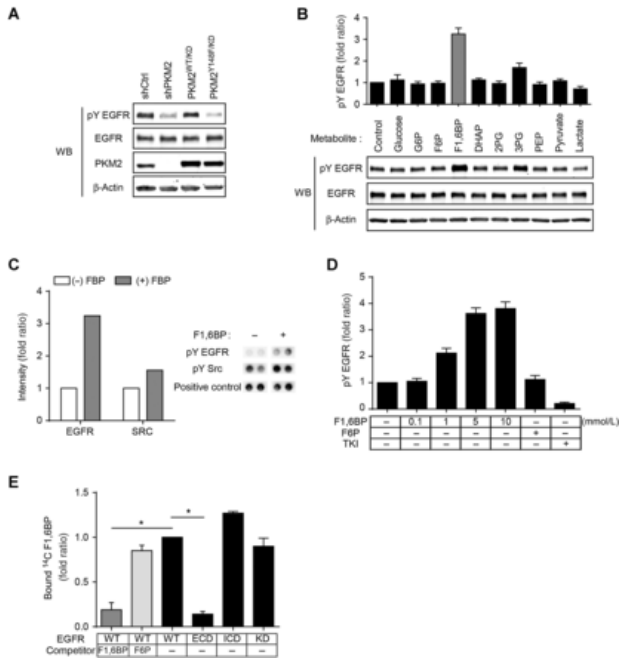

Fig 5: *F1, 6BP enhances EGFR activity through a direct binding with EGFR. A, protein expression of tyrosine-phosphorylated (pY) EGFR in MDA-MB-468 cells expressing control shRNA (shCtrl), sh-PKM2, PKM2$^{WT/KD}$, or PKM2$^{Y148F/KD}$. B, protein expression of pY EGFR in MDA-MB-468 cells treated with various metabolites. Quantification of pY EGFR (top). C, in vitro kinase assay on RTK array with or without 500 µmol/L F1,6BP. Left, quantification of pY EGFR and pY SRC. Right, representative RTK array images of pY EGFR, pY SRC, and positive control. D, quantitation of pY EGFR Western blotting from in vitro EGFR kinase assay on RTK array with the indicated treatments. E, quantification of ^{14}C-F1,6BP–bound EGFR from in vitro binding assay. WT, wild type; ECD, extracellular domain; ICD, intracellular domain; KD, kinase dead mutant.*

Combined inhibition of EGFR and glycolysis synergistically suppresses TNBC cell proliferation

The cross-talk of EGF signaling and glycolysis metabolite prompted us to determine whether blocking of both EGF signaling and glycolysis may be effective in inhibiting cancer cell proliferation. Although 2-DG is one of the most effective inhibitors of glycolysis 2-DG alone is not effective in cancer cell killing and has an unacceptable toxicity at high doses, and gefitinib alone is also not effective in killing breast cancer cells (Fig. 6A). However, we found that gefitinib sensitized TNBC cells to relatively low concentrations of 2-DG (2.5 mmol/L) compared with 2-DG alone (Fig. 6A). The gefitinib–2-DG combination synergistically suppressed cellular proliferation in TNBC cells (MDA-MB-468 and BT549) but not in non-TNBC cells (T47D) compared with each inhibitor alone (Fig. 6A and B and Supplementary Fig. S6A). The combination of gefitinib and another glycolysis inhibitor, 3-bromo-pyruvate (3-BP), also synergistically suppressed TNBC cell proliferation (Fig. 6C and Supplementary Fig. S6B). Remarkably, gefitinib plus 2-DG also significantly reduced tumor volume in an MDA-MB-468 xenograft tumor model in mice (Fig. 6D), indicating that inhibition of both EGFR and glycolysis inhibition has potential as a combination therapeutic approach to treat TNBC.

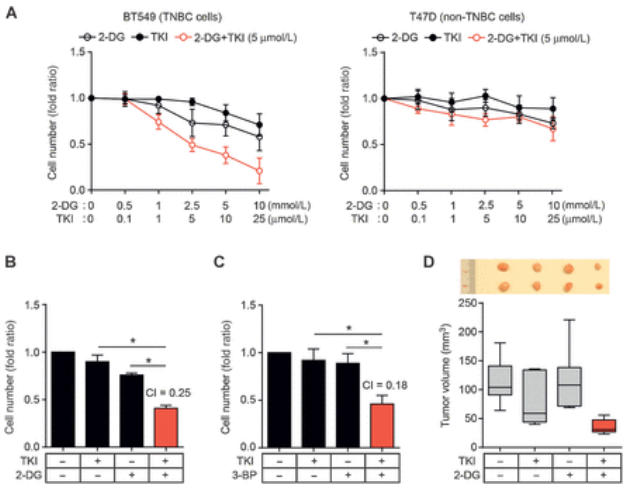

Fig 6: *The combination of EGFR and glycolysis inhibitors synergistically suppresses TNBC cell proliferation. A, proliferation of BT549 (left) and T47D (right) cells treated with glycolysis inhibitor 2-DG and/or TKI as determined by cell counting assay. B and C, proliferation of BT549 cells treated with TKI and/or glycolysis inhibitor 2-DG (B) or 3-BP (C) as measured by cell counting assay. CI, combination index value. CI < 0.8 indicates synergistic effect. D, nude mice were injected with BT549 cells in the mammary glands and treated with 2-DG and/or gefitinib. Tumors were measured and dissected at the endpoint, and tumor size (mm^3) is shown in a box-and-whisker plot.*

EGF signaling–induced production of lactate inhibits cytotoxic T-cell activity

On the basis of our findings that the EGF/EGFR signaling induces glycolytic jam, which leads to the accumulation of glycolytic metabolites in tumor cells and increased extracellular level of lactate (Fig. 1) and a previous report demonstrating that extracellular lactate inhibits cytotoxic T-cell activity we next asked whether extracellular lactate modulates cytotoxic T-cell–related functions in TNBC cells. To this end, we analyzed cytotoxic T-cell activity with or without the addition of lactate by using activated primary

human T cells. Indeed, the population of IFNγ)-positive cytotoxic T cells ($CD8^+$) decreased in culture medium supplemented with lactate (Supplementary Fig. S7). Furthermore, coculture of T cells and $PKM2^{WT}$-expressing MDA-MB-468 cells, which excreted elevated levels of lactate (Fig. 1), had less activated T-cell population accompanied by a decrease in IFNγ and IL2 expression compared with those expressing $PKM2^{Y148F}$ (Fig. 7A and B). Consistently, $PKM2^{WT}$-expressing cells had less T-cell–mediated apoptosis than those expressing $PKM2^{Y148F}$ in a T-cell–mediated tumor cell killing assay (Fig. 7C). The addition of lactate also reduced the number of apoptotic $PKM2^{Y148F}$-expressing cells (Fig. 7C). To further investigate whether this phenomenon occurs *in vivo*, we examined tumor growth, lactate production, and the population of tumor-infiltrating lymphocytes in $PKM2^{WT}$- or $PKM2^{Y148F}$-expressing 4T1 syngeneic BALB/c mouse model because 4T1 cells are commonly used to investigate TNBC in mice. In line with the results from *in vitro* experiments, $PKM2^{WT}$-expressing 4T1 tumors were bigger in mass, and had higher levels of lactate and less activation of cytotoxic T cells compared with those expressing $PKM2^{Y148F}$ (Fig. 7D–F). Together the results suggest that increased levels of extracellular lactate via EGF signaling inhibits cytotoxic T-cell activity, which may contribute to the invasive nature of TNBC cells (Fig. 7G, proposed model).

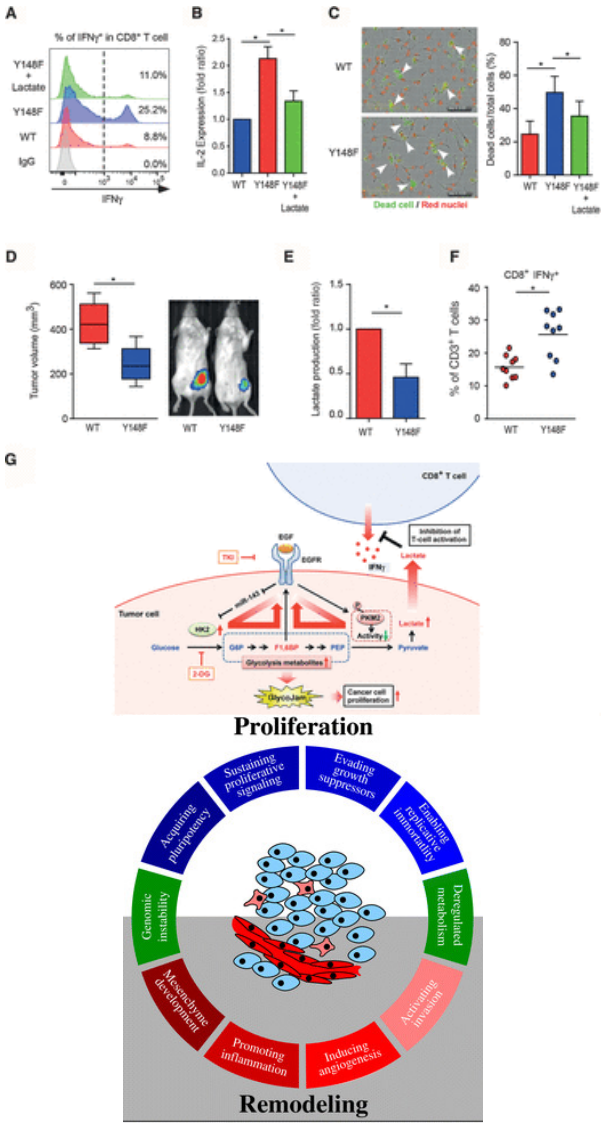

Fig 7: *EGF signaling–induced lactate inhibits cytotoxic T-cell activity. A, flow cytometric analysis of activated cytotoxic T-cell ($IFNγ^+$ and $CD8^+$) population in coculture of primary T cells and $PKM2^{WT}$- or $PKM2^{Y148F}$-expressing MDA-MB-468 cells with or without 10 mmol/L lactate treatment. B, levels of soluble IL2 in coculture of Jurkat T cells and $PKM2^{WT}$- or $PKM2^{Y148F}$-expressing MDA-MB-468 cells. C, representative images from phase contrast microscopy showing red fluorescence (nuclear-restricted RFP) and/or green fluorescence (NucView 488 Caspase 3/7 substrate) from merged images (×20) of $PKM2^{WT}$- or $PKM2^{Y148F}$-expressing MDA-MB-468 cells and activated T cell cocultured in the presence of caspase 3/7 substrate for 96 hours. Scale bar, 10 μm. Green fluorescent cells were counted as dead cells. Right, the percentage of dead cells relative to the total number of cells counted. D, left, tumors were measured and dissected at the endpoint, and tumor size (mm^3) is shown in a box-and-whisker plot. N = 9 mice per group. Right, representative images of tumor growth of $PKM2^{WT}$- or $PKM2^{Y148F}$-expressing mouse 4T1-luc cells in BALB/c mice by IVIS bioluminescence imaging (IVIS100). E, lactate production of $PKM2^{WT}$-or $PKM2^{Y148F}$-expressing 4T1 tumors. F, intracellular cytokine staining of IFNγ in $CD8^+$ $CD3^+$ T-cell populations. $P < 0.05$, two-way ANOVA. N = 9 mice per group. G, proposed model of EGF-mediated glycolytic metabolite accumulation and immune escape.*

Discussion and Conclusion

Tumor cells are known to reprogram their metabolic pathways to fuel cell proliferation, and many oncogenic signaling pathways such as those activated by RTK contribute to this process. Although EGF signaling has been reported to accelerate glucose metabolism in cancer cells, it is not clear whether this is facilitated directly by EGFR. Our current study identifies a mechanism by which EGF signaling mediates aerobic glycolysis through upregulation of HK2 expression, which speeds up the first step of glycolysis, and downregulation of PKM2 activity, which slows down the last step of glycolysis. As a result, this creates a "glycolytic jam" that leads to an accumulation of metabolic intermediates.

In aerobic glycolysis, the switch from PKM1 to PKM2 is a well-recognized metabolic reprogramming event (7, 9). Over the past few years, there has been a substantial increase in our understanding of the molecular mechanism by which PKM2 modulates metabolic rearrangement during cancer progression. In tumorigenesis, cell growth signals stimulate the switch from glycolytically active to inactive PKM2, consequently remodeling the glycolytic pathway to channel the carbon source from glucose for biosynthesis (7, 9). Posttranslational modifications of PKM2, such as phosho-Y105 and acetyl-K305, which decrease PKM2 activity, have been shown to contribute to tumor cell growth. In addition, PKM2 activator promotes a constitutively active state of PKM2 and suppresses tumor cell proliferation. However, a later study demonstrated that the knockdown of PKM2 by siRNA suppresses cell proliferation and tumor growth. These findings point to a contradictory role of PKM2. Although PKM2 is relatively a well-characterized glycolytic enzyme in tumor cells, ligand-stimulated tumorigenic function of PKM2 by protein–protein interaction or posttranslational modification in specific tumor type, such as TNBC, has not been reported. Here, we demonstrated that PKM2 phosphorylation plays an important role in EGF signaling–mediated aerobic glycolysis in TNBC cells.

Until now, metabolites that accumulated via aerobic glycolysis were considered as a building blocks or fuel source for cancer cell proliferation. The loss of fructose-1,6-bisphosphatase (FBP1), which catalyzes the dephosphorylation of F1,6BP to

F6P in gluconeogenesis, was recently determined to be a critical oncogenic event in breast cancer and renal cell carcinoma progression. These findings suggest that F1, 6BP, in addition to serving as a source for cancer cell proliferation, may be important to the regulation of glucose metabolism in cancer. Our findings further support the critical role of F1, 6BP in cancer by modulating oncogenic signaling.

As with glycolytic metabolites, lactate was thought to be just a by-product of glycolysis. However, it was recently shown that lactate functions as an important regulator of cancer development and metastasis through cell-to-cell interactions between cancer, stromal, and endothelial cells. Further studies also demonstrated that extracellular lactate regulates T-cell functions. Here, we provided evidence to support a link between EGF-induced extracellular lactate and cancer cell immune escape through inhibition of cytotoxic T-cell activity. These findings implied that oncogenic signaling of cancer cells regulates not only intracellular metabolic pathway but also extracellular immune escape function.

On the basis of our findings, we propose a model (Fig. 7G) illustrating the effect of oncogenic signaling of EGF/EGFR on aerobic glycolysis and immune escape in TNBC cells. Inhibition of PKM2, the last irreversible step of glycolysis, and upregulation of HK2, the first irreversible step of glycolysis, forms a “glycolytic jam” that results in an accumulation of glycolytic intermediates. Accumulated F1,6BP via this glycolytic jam together with enhanced levels of extracellular lactate contribute to oncogenic signaling, tumor growth, and immune escape. The combined inhibition of EGFR to block oncogenic signaling and of glycolysis to reduce the levels of metabolites may represent a new therapeutic strategy to treat TNBC and possibly other EGFR-expressing cancer cells.

Acknowledgments

All of the authors achieved extreme guidance favoring the in depth cultivation with a positive output from Dr. D.N. Tibarewala, Professor, School of Biosciences and Engineering, Jadavpur University, Kolkata, India. Dr. D.N. Tibarewala contributed a pioneer role to the design of the study, data analysis, and revision of the manuscript. And for that, both of the authors are grateful for his extreme support to make the endeavor successful. Dr. Partha Majumder, being a Human Physiologist and Systems Biologist, contributed major role in order to establish correlation between different metabolic cycle and oncogenic consequences.

References

1. Warburg O On the origin of cancer cells. Science. 1956; 123:309-14.
2. Vander Heiden MG, Cantley LC. Thompson CBUnderstanding the Warburg effect: the metabolic requirements of cell proliferation. Science. 2009; 324:1029-33.
3. Ward PS, Thompson CB. Metabolic reprogramming: a cancer hallmark even warburg did not anticipate. Cancer Cell. 2012; 21:297-308.
4. Dang CV. Links between metabolism and cancer. Genes Dev. 2012; 26:877-90.
5. Fang R, Xiao T, Fang Z, Sun Y, Li F, Gao Y, *et al*. MicroRNA-143 (miR-143) regulates cancer glycolysis via targeting hexokinase 2 gene. J Biol Chem. 2012; 287:23227-35.
6. Mathupala SP, Ko YH, Pedersen PL. Hexokinase II: cancer's double-edged sword acting as both facilitator and gatekeeper of malignancy when bound to mitochondria. Oncogene. 2006; 25:4777-86.
7. Christofk HR, Vander Heiden MG, Harris MH, Ramanathan A, Gerszten RE, Wei R. *et al*. The M2 splice isoform of pyruvate kinase is important for cancer metabolism and tumour growth. Nature. 2008; 452:230-3.
8. Dombrauckas JD, Santarsiero BD, Mesecar AD. Structural basis for tumor pyruvate kinase M2 allosteric regulation and catalysis. Biochemistry. 2005; 44:9417-29.
9. Mazurek S, Boschek CB, Hugo F, Eigenbrodt E. Pyruvate kinase type M2 and its role in tumor growth and spreading. Semin Cancer Biol. 2005; 15:300-8